Effect of Averaging Volume and Algorithm on *In-Situ* Electric Field for Uniform Electric and Magnetic Field Exposures

Akimasa Hirata, Yukinori Takano, Yoshitsugu Kamimura*, Osamu Fujiwara

Nagoya Institute of Technology, Department of Computer Science and Engineering, Japan
* Utsunomiya University, Department of Information Science, Japan

Corresponding Author: Akimasa Hirata
Address: Nagoya Institute of Technology, Gokiso-cho, Showa-ku, Nagoya 466-8555, Japan
Tel&Fax: +81-52-735-7916
E-mail: ahirata@nitech.ac.jp

Abstract

The present study quantified volume-averaged *in-situ* electric field in nerve tissues of anatomically-based numeric Japanese male and female models for exposure to extremely-low-frequency electric and magnetic fields. A quasi-static finite-difference time-domain method was applied to analyze this problem. The motivation of our investigation is that the dependence of electric field induced in nerve tissue on averaging volume/distance is not clear, while a cubical volume of 5×5×5 mm^3 or a straight-line segment of 5 mm is suggested in some documents. The influence of non-nerve tissue surrounding nerve tissue is also discussed by considering three algorithms for calculating averaged *in-situ* electric field in nerve tissue. The computational results obtained herein reveal that volume-averaged electric field in the nerve tissue decreases with the averaging volume. In addition, the 99^{th} percentile value of volume-averaged *in-situ* electric field in nerve tissue is more stable than that of the maximal value for different averaging volume. When including non-nerve tissue surrounding nerve tissue in the averaging volume, resultant *in-situ* electric fields were not so dependent on the averaging volume as compared to the case excluding non-nerve tissue. *In-situ* electric fields averaged over a distance of 5 mm were comparable or larger than that for 5×5×5 mm^3 cube depending on algorithm, nerve tissue considered, and exposure scenarios.

PACS: 87.50.cm

1. Introduction

There has been increasing public concern regarding the adverse health effects associated with electromagnetic fields. Safety guidelines/standards for electromagnetic field exposures have been established by different organizations (ICNIRP 1998, IEEE 2002). One of the most influential guidelines was published by the International Commission on Non-Ionizing Radiation Protection (ICNIRP) (1998). According to the guidelines, the dominant effect of extremely-low frequency (ELF) fields on humans is nerve stimulation due to induced current in the central nerve system (Matthes 1998). Current density averaged over an area of 1 cm^2 is used as a metric of basic restriction. The limit is 10 mA/m^2 for the occupational exposure and 2 mA/m^2 for the general public exposure (ICNIRP 1998).

Recently, *in-situ* electric field has gained significant attention. One of the main reasons for this increasing attention is that the IEEE standards (2002) used *in-situ* electric field averaged over a straight-line segment of 5 mm as a metric for human protection. In addition, Dawson *et al* (1998) reported that the uncertainty of the *in-situ* electric field due to tissue conductivity is much smaller than that of *in-situ* current density. ICNIRP (2009) has opened a draft of new guidelines for time-varying electric and magnetic fields (1 Hz to 100 kHz). According to this draft, *in-situ* electric field averaged over a cube with the side length of 5 mm is used as a metric instead of the current density (ICNIRP 1998). In the computational dosimetry, volume-averaged ($5\times5\times5$ mm^3) *in-situ* electric field was suggested to be used for a practical compromise as Bahr *et al* did (2007). However, a biologically reasonable averaging distance for electric field might extend from 1 to 7 mm (ICNIRP 2009). Then, further research to define the local electric field as an average in a small volume is encouraged since computational results with a voxel model include errors originated from stair-casing approximation.

The purpose of the present study is to investigate the dependence of electric field induced in the nerve tissue on the averaging volume and algorithm in the Japanese adult male and female models named TARO and HANAKO, respectively, (Nagaoka *et al* 2004) for uniform ELF electric and magnetic field exposures. Averaged *in-situ* electric field over a volume of $5\times5\times5$ mm^3 and a straight-line segment of 5 mm are compared in order to obtain some insight on the difference between the metrics prescribed in the draft of ICNIRP (2009) and the IEEE standard (2002).

2. Model and Methods

2.1. Human Phantoms

Whole-body numeric models for the Japanese male (TARO) and the Japanese female (HANAKO) were developed by Nagaoka *et al* (2004). The resolution of these models is 2 mm, and the models are segmented into 51 anatomic regions. The height and weight of TARO are

1.73 m and 65 kg, respectively, whereas those of HANAKO are1.61 m and 53 kg, respectively. Note that the retina is not classified in TARO and HANAKO and thus *in-situ* electric field in the retina is not calculated in the present study.

2.2. Computational Methods

A quasi-static finite-difference time-domain (FDTD) method (De Moerloose *et al* 1997) was used to investigate the induced fields in the anatomic Japanese models. This method extends a conventional FDTD method (Taflove and Hagness 2005) to solve quasistatic problems by choosing incident waveforms appropriately. Under quasistatic approximation, fields exterior to conductors have the same phase as the incident field. The interior fields, on the other hand, are first-order fields that are proportional to the time derivative of the incident field. The incident field is then chosen as a ramp function with a smooth start, as in De Moerloose *et al.* (1997). The cell resolution is chosen as 2 mm so as to coincide with the voxel resolution of the human phantoms.

In order to generate a proper uniform magnetic/electric field, two plane waves in opposite directions were excited so that electric/magnetic fields of the plane waves cancel each other. The computational region is truncated by perfectly matched layers. The conductivities of tissues were chosen on the basis of Gabriel (1996), as listed in Table. 1.

Our computational code has been validated via the intercomparison (Hirata *et al.* 2009b), but for different measures; voxel *in-situ* electric fiend and current density averaged over an area of 1 cm^2. Thus, some comparison with a scalar-potential finite-difference (SPFD) method (Dawson *et al* 1996) was given briefly for further verifying our computational results on volume-averaged *in-situ* electric field.

2.3. Exposure Scenarios

Exposure scenarios considered in the present study are illustrated in Fig. 1. For magnetic field exposure, the human was considered to be standing in free space. Three orientations of magnetic fields were considered: AP (front-to-back), TOP (top-to-bottom), and LAT (side-to-side). The frequency and magnitude of the magnetic flux density are 50 Hz and 1 mT, respectively. For electric field exposure, the human was considered to be standing on the perfect conductor. The orientation of electric field is top-to-bottom (TOP). The frequency and magnitude of the electric field are 50 Hz and 1kV/m, respectively.

2.4. Post-Processing of *In-Situ* Electric Field

A suggested averaging volume of *in-situ* electric field in the draft of the ICNIRP guidelines (2009) is a cube of its side length of 5 mm. Averaged *in-situ* electric field is calculated for each

voxel which is assigned to nerve tissue. Specifically, such voxels are considered as reference points for applying a post-processing algorithm which will be given below. Side length of the averaging volume was varied in order to investigate the effect of averaging volume/distance on the *in-situ* electric field. When a side length of the cube does not coincide with the voxel resolution, we used a linear interpolation to calculate averaged *in-situ* electric field.

A detailed procedure for computing *in-situ* electric field is not prescribed in the draft of the ICNIRP guidelines (2009) as well as the ICNIRP guidelines (1998) and IEEE standard (2002). In that draft, the paper by Bahr *et al* (2007) is referenced, in which they computed one voxel value of *in-situ* electric field for the model resolution of 5 mm. This value may be considered as one of the following algorithms which compute the average value only when the averaged volume is comprised of nerve tissue only. However, the model resolution is limited to 5 mm, although the model resolution developed recently is 2 mm or less. In addition, the resolution of 5 mm is insufficient to represent nerve tissue, such as retina. The inclusion of non-nerve tissue in the averaging region is discussed for induced current density over 1 cm^2 (e.g., A. Hirata et al 2001, Dimbylow 2008, Zoppetti and Andreucetti 2009). This scheme is based on the response of ICNIRP (1999) to CENELEC, which suggests that, for the purpose of simplification, it is acceptable to assume that the 1-cm^2 sections are composed entirely of nerve tissue. This description is not on electric filed but on current density. However, we applied this idea to *in-situ* electric field. Then, the following three algorithms were considered.

The first algorithm (*i*) is that any tissue is allowed in the averaging volume as far as the central voxel in the averaging region is assigned to nerve tissue. The second algorithm (*ii*) is that averaged *in-situ* electric field is calculated by assuming that electric filed in non-nerve tissue is zero. Furthermore, as the third algorithm (*iii*), the averaged *in-situ* electric field is computed only when averaged volume comprised entirely of nerve tissues.

In the same manner, these algorithms are applied to the averaged *in-situ* electric field over a straight-line segment of 5 mm, which is a metric prescribed in the IEEE standard (2002). The averaging distance is not a multiple of the model resolution and thus a linear interpolation was applied. At each voxel of nerve tissue, the 5-mm averaged electric field is calculated for *x*, *y*, and *z* directions. Then, the maximum values of these three values are considered as *in-situ* electric field of the voxel.

The 99-*th* percentile value of voxel and volume-averaged *in-situ* electric fields are computed, even though it is noted to be arbitrary (ICNIRP 2009). The 99-th percentile voxel field was first introduced by a group of University of Victoria for avoiding computational uncertainty attributed to stair-casing approximation of voxel human phantoms (Dawson *et al* 2001). The rationale for this measure is that, in a multi-layer sphere, the 99-th percentile electric field computed by the FDTD method and the maximum value of an analytical solution are in good

agreement. This coincidence is caused by excluding singular behavior of the FDTD-computed field in voxel model. Even though the effectiveness of this measure cannot be evaluated in the anatomically based model, this measure is often used (e.g., Hirata *et al* 2001). Dan Bracken and Dawson (2004) showed that, for spheres and ellipsoids, the 99-th value of averaged *in-situ* electric field over 1 cm^2 with the FDTD method is in better agreement with an analytical solution than the 99th percentile value of voxel electric field. This is the main reason for presenting the 99^{th} percentile value of *in-situ* electric field averaged over a specific volume in addition to the voxel value. The same conclusion has been reported by Yamazaki *et al* (2007). When the non-nerve tissue was included in the averaging volume for the algorithm (iii), the averaged in-situ electric field is considered as 0 in our study.

3. Computational Results

In order to validate computational results of volume-averaged *in-situ* electric field with the FDTD method, first, the results computed with the FDTD method and the SPFD method (Dawson and Stuchly, 1996) are compared for exposure to magnetic field. In this comparison, the algorithm (*i*) for the AP direction was considered. The maximum value of voxel *in-situ* electric field in the brain and spinal cord by the FDTD method were 69.8 mV m^{-1} and 82.7 mV m^{-1} (see Table 2) while they were 70.1 mV m^{-1} and 73.4 mV m^{-1} by the SPFD method. Similarly, the maximum *in-situ* electric field averaged over 6×6×6 mm^3 cube in the brain and spinal cord by the FDTD method were 43.7 mV m^{-1} and 56.1 mV m^{-1} while 52.3 mV m^{-1} and 43.2 mV m^{-1} by the SPFD method. Their 99th percentile values are in better agreement with each other as than the maximum value. Specifically, the 99th percentile value of electric field in the brain and spinal cord averaged over 6×6×6 mm^3 cube by the FDTD method were 24.6 mV m^{-1} and 26.7 mV m^{-1} (see Table 2) while they were 25.4 mV m^{-1} and 27.2 mV m^{-1} by the SPFD method. These differences are comparable to those reported in Hirata et al (2009b) for different measures, mainly on the current density.

Table 2 lists the dependence of *in-situ* electric field in the brain and spinal cord on the averaging volume with three algorithms. As seen from Table 2, the *in-situ* electric fields become smaller with the averaging volume. Some discrepancy, however, was observed in the averaged fields with (*i*). *In-situ* electric fields with (*i*) are less sensitive to the averaging volume than that with (*ii*). Specifically, for magnetic field exposure with AP direction, the ratio of voxel electric field ($2\times2\times2$ mm^3) to that for $10\times10\times10$ mm^3 in the brain is 1.7 for (*i*) and 2.5 for (*ii*) while that in the spinal cord is 1.8 for (*i*) and 4.2 for (*ii*). The result for (*iii*) is identical to or somewhat smaller than that for (*ii*). The same tendency was observed for magnetic field exposure with the other directions and electric field exposure.

From the same table, the 99-*th* percentile value of *in-situ* electric field was less dependent on

averaging volume than the maximum value. Specifically, for magnetic field exposure with the AP direction, the ratio of averaged *in-situ* electric field in the brain over $2\times2\times2$ mm^3 to that for $10\times10\times10$ mm^3 for the algorithm (*i*) is 1.73 for the maximum value while 1.2 for the 99-th percentile value. The same tendency was observed for magnetic field exposures with the other directions and electric field exposure. Note that the 99-th percentile value for the algorithm (*iii*) becomes smaller for larger averaging volume, since the condition that the whole volume should comprise entirely of nerve tissues is not satisfied.

Table 3 (a) lists the *in-situ* electric fields in HANAKO for magnetic-field exposure with AP direction. From this table, a similar tendency was observed between male and female models with respect to the maximum and 99th percentile values of the *in-situ* electric field. However, the maximum and 99th percentile values in the brains of HANAKO were smaller than those of TARO by 35% or less, which is attributed to the difference in the circumstances of the phantom (Dimbylow 2005, Hirata *et al* 2009a). The results for HANAKO exposed to magnetic field with the other directions are not presented here for avoiding repetition, since the same tendency was observed. As seen from Table 3 (b), for electric field exposure, *in-situ* electric fields of TARO and HANAKO are comparable to each other, which coincide with the tendency reported by Dimbylow (2005). The *in-situ* electric field is approximately proportional to the square of the height divided by the horizontal cross area (Deno and Zaffanell 1982).

Table 4 lists *in-situ* electric field averaged over a straight-line segment of 5 mm (IEEE, 2002) in order to clarify the difference with *in-situ* electric field averaged over 5×5×5 mm^3 cube. As discussed above, the results with the algorithm (*iii*) is almost identical to those with (*ii*). This tendency is more remarkable for a straight-line segment than that for the cube. Thus, the results with the algorithms (*i*) and (*ii*) only are presented in this table. As seen from Table 4, the difference between *in-situ* electric field averaged over a straight-line segment of 5 mm and 5×5×5 mm^3 cube are smaller than 40%. For the algorithm (ii), averaged *in-situ* electric field over the straight-line segment of 5 mm provide the larger value than that for the averaging volume of are 5×5×5 mm^3, since more voxels with non-nerve tissue are included in the cube 5×5×5 mm^3.

4. Discussion and Summary

The present study investigated the effect of averaging scheme and averaging volume/distance on averaged *in-situ* electric field. The algorithm (*i*) provided the largest value. This is caused by the inclusion of tissue whose conductivity is relatively low, such as the bone, resulting in higher field to satisfy the continuity of the current. For the algorithm (*ii*), some region whose *in-situ* electric field is relatively large must be excluded due to the restriction of the algorithm. The algorithm (*iii*) is applied only when all the voxels in the averaging volumes are assigned to

nerve tissue. Thus, computed *in-situ* electric field was the same or somewhat smaller than those with (*ii*).

The motivation for investigating the effect of averaging volume is that a biologically reasonable averaging distance for electric field might extend from 1 to 7 mm, while a cube with the side length of 5 mm is used as a metric in the draft guidelines of ICNIRP (2009). From our comparisons, the *in-situ* electric field with the averaging algorithm (*i*) is less sensitive to the averaging volume than that with (*ii*). As the resolution of the model is limited to 2 mm, we could not compute *in-situ* electric field at the resolution of 1 mm. However, the difference of *in-situ* electric fields with the cube of 2 mm and 8 mm was by a factor of 2 or more. This difference was larger for the algorithms (*ii*) and (*iii*). When considering the 99^{th} value of averaged *in-situ* electric field, the difference was at most a few tens percents.

Different metrics, *in-situ* electric field averaged over the cube 5×5×5 mm^3 and distance of 5 mm are used in different guidelines/standards (IEEE 2002, ICNIRP 2009). The difference between the maximum value of *in-situ* electric fields over the distance of 5 mm and that over 5×5×5 mm^3 was marginal for the algorithm (*i*) while the latter is smaller than that in the former in some cases due to larger averaging region.

Finally, let us comment the measure of 99^{th} percentile value of *in-situ* electric field. The rationale for introducing the 99^{th} percentile value instead of the maximal value in the computation was that better agreement was obtained between 99^{th} percentile value of FDTD-calculated field and analytically maximum field for a two-layer sphere (Dawson *et al* 2001). Our attention focuses on *in-situ* electric field in nerve tissue which appears at tissue boundary. The dominant factor influencing the accuracy at tissue interface is attributed to the contrast of conductivity. The contrast in the conductivity between nerve tissue and surrounding tissue is the order of 5-10 (see Table 1). According to Dawson *et al* (2001), for a two-layer sphere with the resolution of 3.6 mm, the enhancement of singular behavior at the stair-casing approximation was reported to be 12%-21% for magnetic-field exposure and 89% for electric-field exposure, while the 99^{th} percentile value is in good agreement with the analytical solution. The differences between maximum and 99^{th} percentile values observed in the present study are much larger than those in Dawson *et al* (2001). Possible reason for this discrepancy would be the anatomical configuration of the model. Further discussion is impossible since no analytical solution exists for anatomically based phantoms.

References

Bahr A, Bolz T, and Hennes C. 2007 Numerical dosimetry ELF: accuracy of the method, variability of models and parameters, and the implication for quantifying guidelines *Health Phys* 521-530.

Cech R, Leitgeb N and Pediaditis. 2007 Fetal exposure to low frequency electric and magnetic fields *Phys. Med. Biol.* **52** 879–88

Dan Bracken T and Dawson T. 2004 Evaluation of nonuniform 60-Hertz magnetic-field exposures for compliance with guidelines *J. Occupatinal Environ Hygiene* **1** 629-638

Dawson T W and Stuchly M A 1996 Analytic validation of a three-dimensional scalar-potential finite-difference code for low-frequency magnetic induction *Appl. Comput. Electromagnet. Soc. J* **11** 63-71

Dawson T W, Caputa K, Stuchly M A. 1998 Effects of skeletal muscle on human organ dosimetry under 60 Hz uniform magnetic field exposure. *Phys. Med. Biol.* **43** 1059-1074

Dawson T W, Potter M and Stuchly M A. 2001 Evaluation of modeling accuracy of power frequency field interactions with the human body *ACES Journal* 16 162-72

DeMoerloose J, Dawson T W and Stuchly M A. 1997 Application of FDTD to quasi-static field analysis *Radio. Sci.* **8** 355-75

Deno D W and Zaffanell L E 1982 Field effects of overhead transmission lines and stations (in Transmission Line Reference Book: 345 kV and above, 2nd Ed) Palo Alto, CA:EPRI 329-419

Dimbylow P J. 2000 Current densities in a 2 mm resolution anatomically realistic model of the body induced by low frequency electric fields *Phys. Med. Biol.* **45** 1013-22

Dimbylow P. 2005 Development of the female voxel phantom, NAOMI, and its application to calculations of induced current densities and electric fields from applied low frequency magnetic and electric fields *Phys. Med. Biol.* **50** 1047-70

Dimbylow P. 2006 Development of pregnant female, hybrid voxel-mathematical models and their application to the dosimetry of applied magnetic and electric fields at 50 Hz *Phys. Med. Biol.* **51**, 2383-94

Dimbylow P. 2008 Quandaries in the application of the ICNIRP low frequency basic restriction on current density *Phys. Med. Biol.* **53** 133-45

Gabriel S, Lau R W, and Gabriel C 1996 The dielectric properties of biological tissues: III. Parametric models for the dielectric spectrum of tissues *Phys. Med. Biol.* **41** 2271-293

Hirata A, Caputa K, Dawson T W, and Stuchly M 2001 Dosimetry in models of child and adult for low-frequency electric field *IEEE Trans Biomed Eng* **48** 1007-12

Hirata A, Wake K, Watanabe S, and Taki M 2009a In-situ electric field and current density in Japanese male and female models for a uniform magnetic field exposures *Rad. Prot. Dosimetry* **135** 272-5

Hirata A, Yamazaki K, Hamada S, Kamimura Y, Tarao H, Wake K, Suzuki Y, Hayashi Nand Fujiwara M 2009b Intercomparison of induced fields in Japanese male model for ELF magnetic field exposures: effect of different computational methods and codes *Rad. Prot. Dosimetry* **(**doi:10.1093/rpd/ncp251**)**

ICNIRP. 1998 Guidelines for limiting exposure to time-varying electric, magnetic, and electromagnetic fields (up to 300 GHz)., *Health Phys.* 74, 494-522

ICNIRP. 1999 Response to CENELEC Working Group Convenor. CENELEC TC106X online document archive. Document TC106X/Chair/0006/INF

ICNIRP. 2009 Draft Guidelines for limiting exposure to time-varying electric and magnetic fields (1 Hz to 100 kHz). http://www.icnirp.de/openELF/ICNIRPConsultationELF0709.pdf

Matthes R. Response to questions and comments on ICNIRP *Health Phys*. 75, 438-9 (1998).

Nagaoka T, Watanabe S, Sakurai K, Kunieda E, Watanabe S, Taki M and Yamanaka Y. 2004 Development of realistic high-resolution whole-body voxel models of Japanese adult males and females of average height and weight, and application of models to radio-frequency electromagnetic-field dosimetry *Phys. Med. Biol.* 49, 1-15

Taflove A and Hagness S. 2003 Computational Electrodynamics: The Finite-Difference Time-Domain Method: 3rd Ed. Norwood. MA: Artech House

Yamazaki K, Kawamoto T, Fujinami H, and Shigemitsu T 2007 On the method of investigating human exposure to nonuniform magnetic field *Trans. IEEJ* **127** 239-247

Zoppetti N and Andreuccetti. 2009 Influence of the surface averaging procedure of the current density in assessing compliance with the ICNIRP low-frequency basic restrictions by means of numerical techniques *Phys. Med. Biol.* 4835-4848.

Table 1. Conductivity of human tissue [S/m].

tissues	S/m	tissues	S/m
cerebellum	0.10	pancreas	0.35
C.S.F.	2.00	prostate	0.40
cornea	0.40	small intestine	0.50
eye humor	1.50	spleen	0.10
grey matter	0.10	stomach	0.50
hypothalamus	0.08	stomach contents	0.35
eye lens	0.25	tendon	0.30
pineal body	0.08	testis	0.35
pituitary	0.08	thyroid gland	0.50
salivary gland	0.35	trachea	0.35
thalamus	0.08	urine	0.70
tongue	0.30	blood	0.70
white matter	0.06	cortical bone	0.02
adrenals	0.35	bone marrow	0.06
bladder	0.20	cartilage	0.18
large intestine	0.10	fat	0.04
duodenum	0.50	muscle	0.35
esophagus	0.50	nerve(spinal cord)	0.03
bile	1.40	skin	0.10
gall bladder	0.20	tooth	0.02
heart	0.10	ligament	0.30
kidney	0.10	diaphragm	0.35
liver	0.07	seminal vesicle	0.35
lung	0.14	cavernous body	0.35
large intestine contents	0.35	small intestine contents	0.35

Table 2. *In-situ* electric field exposure in brain and spinal cord of TARO for magnetic field exposure with (a) LAT, (b) AP and (c) TOP directions, and for electric field exposure with TOP direction. The frequency is 50 Hz. The magnitude of magnetic flux density is 1 mT for (a), (b), and (c) and 1 kV/m for (d). The unit of *in-situ* electric field has mV m^{-1}.

(a)

			Averaging volume [mm cubic]					
		algorithm	2	4	5	6	8	10
Brain	max	(i)	67.2	41.4	39.9	38.8	39.2	38.0
		(ii)	67.2	36.0	35.7	35.8	32.1	32.0
		(iii)	67.2	36.0	35.7	35.8	32.1	32.0
	99th	(i)	28.5	26.2	26.0	26.0	25.0	24.7
		(ii)	28.5	25.3	25.1	24.9	23.6	23.2
		(iii)	28.5	24.5	24.5	24.5	21.5	21.4
Spinal cord	max	(i)	86.9	44.8	40.2	38.0	32.1	31.5
		(ii)	86.9	40.9	37.3	35.2	29.5	28.7
		(iii)	86.9	34.2	34.4	35.2	27.3	27.3
	99th	(i)	37.7	30.7	30.1	29.7	27.7	26.7
		(ii)	37.7	27.1	26.5	26.2	23.6	22.3
		(iii)	37.7	23.3	23.4	23.4	4.5	4.5

(b)

			Averaging volume [mm cubic]					
		algorithm	2	4	5	6	8	10
Brain	max	(i)	69.8	41.7	42.8	43.7	41.3	40.3
		(ii)	69.8	34.0	33.6	33.4	28.2	27.5
		(iii)	69.8	34.0	33.6	33.4	27.7	27.4
	99th	(i)	25.3	23.2	23.1	23.1	22.2	21.9
		(ii)	25.3	22.0	21.7	21.6	20.5	20.0
		(iii)	25.3	21.2	21.1	21.1	18.3	18.2
Spinal cord	max	(i)	82.7	62.7	58.7	56.1	49.3	46.6
		(ii)	82.7	32.6	31.7	30.8	22.5	19.7
		(iii)	82.7	26.2	26.6	26.9	17.5	17.7
	99th	(i)	30.2	27.6	27.0	26.7	26.3	26.2
		(ii)	30.2	20.1	19.7	19.4	16.9	15.9
		(iii)	30.2	15.2	15.4	15.3	2.0	2.0

(c)

			Averaging volume [mm cubic]					
		algorithm	2	4	5	6	8	10
Brain	max	(i)	52.8	32.2	30.8	30.5	24.7	23.0
		(ii)	52.8	28.8	28.2	27.8	21.6	21.2
		(iii)	52.8	28.8	28.2	27.8	21.1	21.2
	99th	(i)	21.4	19.4	19.2	19.1	17.9	17.4
		(ii)	21.4	18.4	18.1	17.9	16.3	15.7
		(iii)	21.4	17.2	17.1	17.1	13.8	13.8
Spinal cord	max	(i)	54.8	40.5	37.5	35.5	30.8	28.3
		(ii)	54.8	17.2	16.1	15.9	11.0	10.7
		(iii)	54.8	13.3	13.5	13.6	10.1	10.1
	99th	(i)	21.7	20.1	20.1	20.1	18.7	18.0
		(ii)	21.7	12.9	12.0	11.6	9.3	8.7
		(iii)	21.7	8.0	8.2	8.3	2.2	2.2

(d)

			Averaging volume [mm cubic]					
		algorithm	2	4	5	6	8	10
Brain	max	(i)	2.86	1.87	2.00	2.12	1.69	1.65
		(ii)	2.86	1.74	1.71	1.71	1.37	1.24
		(iii)	2.86	1.71	1.71	1.71	1.24	1.24
	99th	(i)	1.28	1.16	1.14	1.14	1.07	1.05
		(ii)	1.28	1.11	1.10	1.09	1.02	1.00
		(iii)	1.28	1.07	1.06	1.06	0.93	0.93
Spinal cord	max	(i)	7.81	4.00	3.39	3.10	2.51	2.36
		(ii)	7.81	3.63	3.09	2.91	2.31	2.17
		(iii)	7.81	2.87	2.79	2.73	2.07	2.06
	99th	(i)	3.36	2.45	2.37	2.36	2.18	2.10
		(ii)	3.36	2.19	2.13	2.10	1.83	1.71
		(iii)	3.36	1.83	1.82	1.83	0.64	0.65

Table 3. *In-situ* electric field in brain and spinal cord of HANAKO for magnetic field exposure with (a) AP direction and for electric field exposure with TOP direction. The frequency is 50 Hz. The magnitude of magnetic flux density is 1 mT for (a) and the magnitude of electric field is 1 kV/m for (b). The unit of *in-situ* electric field has mV m^{-1}.

(a)

			Averaging volume [mm cubic]					
		algorithm	2	4	5	6	8	10
Brain	max	(i)	53.6	38.9	38.7	38.6	32.1	29.7
		(ii)	53.6	29.9	29.5	29.4	24.0	23.5
		(iii)	53.6	29.9	29.5	29.4	24.0	23.5
	99th	(i)	24.3	22.0	21.8	21.6	20.6	20.3
		(ii)	24.3	20.8	20.5	20.4	18.9	18.3
		(iii)	24.3	20.0	19.9	19.8	16.9	16.8
Spinal cord	max	(i)	29.4	25.8	25.5	25.4	26.1	26.5
		(ii)	29.4	11.7	9.4	9.3	7.9	7.4
		(iii)	29.4	9.4	9.3	9.3	5.3	5.5
	99th	(i)	11.0	9.9	9.8	9.7	10.9	12.2
		(ii)	11.0	7.9	7.6	7.4	6.0	5.3
		(iii)	11.0	6.3	6.3	6.3	1.9	1.9

(b)

			Averaging volume [mm cubic]					
		algorithm	2	4	5	6	8	10
Brain	max	(i)	3.01	2.78	2.98	3.11	2.74	2.84
		(ii)	3.01	1.91	1.89	1.88	1.66	1.56
		(iii)	3.01	1.91	1.89	1.88	1.38	1.37
	99th	(i)	1.33	1.18	1.16	1.16	1.12	1.13
		(ii)	1.33	1.12	1.10	1.09	1.04	1.02
		(iii)	1.33	1.08	1.08	1.07	0.97	0.97
Spinal cord	max	(i)	6.39	3.97	3.78	3.67	3.14	2.91
		(ii)	6.39	2.81	2.77	2.83	1.99	1.80
		(iii)	6.39	2.81	2.77	2.83	1.12	1.14
	99th	(i)	2.72	2.41	2.35	2.31	2.19	2.17
		(ii)	2.72	1.78	1.73	1.70	1.39	1.24
		(iii)	2.72	1.59	1.59	1.59	0.86	0.86

Table 4. Maximum *in-situ* electric field in brain and spinal cord of (a) TARO and (b) HANAKO for the same condition in Table 2. The field was averaged over distance of 5 mm. The unit of *in-situ* electric field has mV m^{-1}.

(a)

		magnetic field			electric field
	algorithm	LAT	AP	TOP	TOP
Brain	(i)	67.8	42.5	31.4	1.94
	(ii)	37.3	39.3	31.4	1.76
Spinal cord	(i)	39.5	50.7	32.9	3.35
	(ii)	39.5	35.2	23.1	3.25

(b)

		magnetic field			electric field
	algorithm	LAT	AP	TOP	TOP
Brain	(i)	49.3	34.5	27.2	2.58
	(ii)	37.5	34.5	25.2	1.87
Spinal cord	(i)	40.4	24.0	20.1	3.54
	(ii)	29.8	22.1	19.0	3.42

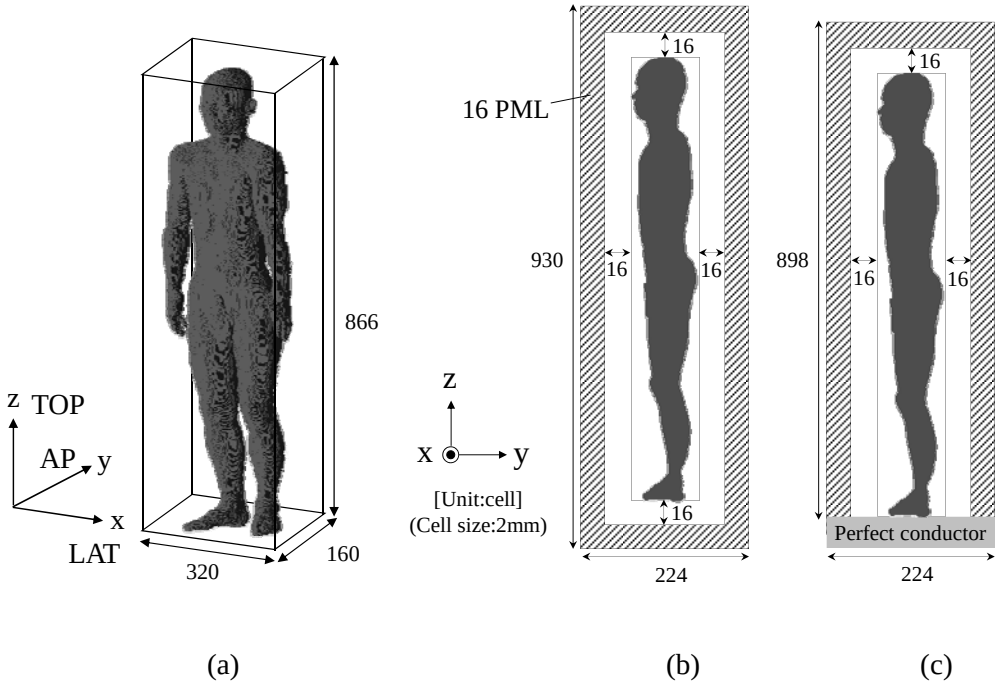

Figure 1: Schematic explanation of (a) definition of coordinates and exposure directions, and FDTD computational domain for (b) magnetic-field and (c) electric-field exposures.